Johan *et al. AMB Express* (2025) 15:155
https://doi.org/10.1186/s13568-025-01966-7

AMB Express

RESEARCH Open Access

Methanol response of V171S lipase from *Geobacillus* sp. 42 explored via experimental and in silico approaches

Ummie Umaiera Mohd Johan[1,2], Siti Nor Hasmah Ishak[1], Wahhida Latip[1], Raja Noor Zaliha Raja Abd. Rahman[1], Abu Bakar Salleh[1], Adam Thean Chor Leow[1,3] and Mohd Shukuri Mohamad Ali[1,2*]

Abstract

The stability of lipase in organic solvents is crucial for biocatalytic processes in industrial biotechnology. Previously, we described a thermostable and solvent-tolerant Lip 42 from *Geobacillus* sp. Despite these features, the wild-type Lip 42 activity deteriorated and became unstable in methanol at high temperatures, limiting its effectiveness in solvent-driven catalysis. This study aims to integrate experimental data with molecular dynamics simulation, free energy landscape (FEL), and principal component analysis (PCA) to explore the structural and dynamic properties of V171S mutant lipase, in aqueous and methanol environments. Optimal conditions were determined at pH 8.0 and 70 °C, with notable thermal stability at 65 °C. Importantly, V171S exhibited solvent tolerance, maintaining over 70% relative activity in methanol, ethanol, acetone, 1-propanol, heptanol, octanol, and n-hexane. To further evaluate its performance in methanol, comparative in silico analyses were performed against the wild-type lipase. Structural analysis revealed that V171S maintained stability with only minor fluctuations compared to the native Lip 42 in methanol condition at 65 °C. Root mean square fluctuation (RMSF) analysis highlighted increased flexibility in the lid 1 region, suggesting structural adaptation to solvent exposure. The principal component analysis demonstrated that Lip 42 adopted broader structural distributions in methanol compared to the V171S variant. Free energy landscape analysis confirmed the presence of distinct and stable energy minima for V171S in methanol. Collectively, V171S mutation improves structural integrity under methanol stress, especially at high temperatures. This study contributes to the development of robust biocatalysts that function efficiently in mixed-solvent systems operating at elevated temperatures, especially in the field of biodiesel production.

Keywords Lipase, Organic solvent tolerance, Molecular dynamic simulations, Free energy landscape, Principal component analysis

*Correspondence:
Mohd Shukuri Mohamad Ali
mshukuri@upm.edu.my
[1]Enzyme and Microbial Technology Research Centre, Faculty of Biotechnology and Biomolecular Sciences, Universiti Putra Malaysia, 43400 Serdang, Selangor, Malaysia
[2]Department of Biochemistry, Faculty of Biotechnology and Biomolecular Sciences, Universiti Putra Malaysia, 43400 Serdang, Selangor, Malaysia
[3]Department of Cell and Molecular Biology, Faculty of Biotechnology and Biomolecular Sciences, Universiti Putra Malaysia, Serdang, Selangor, Malaysia

Introduction

Lipases (EC 3.1.1.3) are ubiquitous hydrolases present in many organisms and catalyze the breakdown of esters and triacylglycerides into fatty acids and glycerol. In a micro water environment, lipases can catalyze the synthesis reaction for interfacial activation (Qin et al. 2023). Additionally, lipases exhibit positional or random specificity toward hydrolysis and synthesis reactions (Albayati et al. 2020). Because of these distinguishing features, lipase has the potential to be an outstanding biocatalyst in a variety of practical applications. Thermostable lipases from thermophiles are especially appealing since industrial processes frequently demand harsh, high-temperature operating conditions. Recently, lipases have been increasingly used in non-aqueous environments such as methanol and ethanol for transesterification in biodiesel production (Salgado et al. 2022). Alcohols become more miscible with oil at higher temperatures, promoting a more uniform reaction environment and potentially reducing the overall reaction time. These factors can contribute to higher productivity and faster biodiesel conversion. However, high temperatures also pose significant challenges, especially to the stability of enzymes. Many lipases are sensitive to heat and may destabilize due to the disruption of structural interactions. Protein engineering approaches, such as rational design and directed evolution, are powerful tools for diversifying enzyme functions and characteristics. Site-directed mutagenesis has successfully enhanced the catalytic efficiency and stability of several enzymes. Site-directed mutation of G210C on lipase from *Staphylococcus epidermidis* AT2 (rT-M386) successfully enhanced the catalytic activity and thermostability, exhibited an optimal temperature switch from 25 to 45 °C and stability up to 50 °C (Veno et al. 2019). Min et al. (2021) successfully improved the characteristic of lipase from *Bacillus subtilis* in water-ethanol solvent via rational surface engineering with 50% of activity remaining. Additionally, mutant *Thermomyces lanuginosus* lipase (TLL) demonstrated significantly improved thermostability and catalytic efficiency with a higher yield in fatty acid methyl esters (FAME), making it suitable for biodiesel production (Qu et al. 2024).

One unique property that lipase has as compared to other lipolytic enzymes is the presence of the lid domain. The structure of this mobile subdomain profoundly impacts the enzyme properties, by altering the open and closed conformation at lipid-water interfaces which reflects the active and inactive state of the enzyme. The key aspects of lid structure that affect lipase stability and functionality are the flexibility, rigidity and amino acid sequence. Hence, the lid is an attractive region for protein engineering in order to understand its dynamic and altered properties. Protein motions and conformational changes can be studied with the help of molecular dynamics (MD) simulations (Padhi et al. 2022). This computational tool enables the atomistic insights of the enzyme and the observation of dynamic processes over time (Radkiewicz and Brooks 2000; Wand and Sharp 2018; Khan et al. 2020). Previously, solvent-tolerant lipase Lip 42 of thermostable *Bacillus* sp. strain 42 (Accession number: AY 78735) was isolated locally from palm oil mill effluent (Eltaweel et al. 2005). Recombinant Lip 42 was successfully purified using the Strep-tag II affinity tag and well characterized. Lipase Lip 42 is a thermostable lipase with optimum catalytic activity at 70 °C. The wild-type Lip 42 retained high activity in various organic solvents, including methanol, at moderate temperatures. However, when Lip 42 was exposed to methanol at a temperature of 60 °C, the residual activity decreased dramatically (Hamid et al. 2009a). A single-point mutation using rational design on a residue located at the lid was performed, namely V171S lipase, to understand the role of hydrophobic interaction for the interfacial activation of lipase in solvents, particularly DMSO (Hamid et al. 2009 b).

In this study, we first presented the biochemical characterization of V171S mutant lipase to understand the mutation impact on its stability and functionality. In biodiesel production, methanol serves as the common solvent used in transesterification reaction between triglycerides and alcohol. Considering the growing interest in lipases as biocatalysts in biodiesel field, the behavior of the V171S mutant was specifically investigated under methanol-containing conditions through detailed kinetic simulation analysis (Almeida et al. 2021). Taken together the experimental data and the in silico studies, V171S mutant lipase demonstrated an improvement in methanol tolerance.

Materials and methods

Purification of V171S mutant lipase

E. coli BL21(DE3)pLysS harbouring pET51b/V171S was obtained from Enzyme and Microbial Technology Research Centre (EMTech), Universiti Putra Malaysia. Previously, site-directed mutagenesis was performed on recombinant plasmid pET51b harboring the lip42 gene using the QuikChange kit (Stratagene, USA). Specific forward and reverse primers were designed to substitute Val171 with Ser and the presence of the V171S mutation was confirmed by DNA sequencing (Hamid et al. 2009b). The V171S mutant lipase was purified to homogeneity by affinity chromatography as described by Hamid et al. (2009a, b). The purified protein was analyzed by sodium dodecyl sulphate-polyacrylamide gel electrophoresis (SDS-PAGE) according to Laemmli (1970).

Lipase assay and protein determination

The hydrolysis of lipase to liberate free fatty acids was determined calorimetrically according to Kwon and Rhee (1986), using olive oil as the substrate. A mixture containing 2.5 mL of substrate (1:1 of olive oil and Tris-HCl buffer at pH 8.0 ratio), 20 µL of 20 mM $CaCl_2$, 10 µL protein sample, and 990 µL Tris-HCl buffer pH 8.0 was incubated in a water bath shaker at 70 °C for 30 min with agitation at 200 rpm. 1 mL of 6 M HCl and 5 mL of isooctane were added to the reaction mixture and homogenized for 30 s with a vortex mixer. After allowing the solvent mixture to separate, 4 mL of the upper layer containing the fatty acids was pipetted into a test tube. Cupric acetate-pyridine reagent (1 mL) was added and the mixtures were vortexed for 30 s. Subsequently, the mixture was incubated at room temperature for 2 h until the aqueous phase separation of isooctane and free fatty acid was observed. The amount of free fatty acid was determined by measuring the product at an absorbance of 715 nm. One unit of lipase activity was defined as the rate of liberation of 1 µmol fatty acid released per min at 70 °C assay condition.

The Bradford method was used to determine the protein concentration, using the Bradford reagent from Supelco® (Sigma-Aldrich) with bovine serum albumin (BSA: Sigma, USA) as the standard (Bradford 1976).

Characterisation of V171S mutant lipase

Optimal temperature and thermal stability

The optimum temperature profile of the mutant lipase was determined at temperatures ranging from 30 °C to 80 °C (5 °C intervals). The assay mixture containing 2.5 mL of substrate (1:1 of olive oil and Tris-HCl buffer at pH 8.0 ratio), 20 µL of 20 mM $CaCl_2$, 10 µL protein sample, and 990 µL Tris-HCl buffer pH 8.0 was incubated in a water bath shaker for 30 min with agitation at 200 rpm. The optimum activity was recorded as 100% relative activity.

For lipase stability study, lipase was pre-incubated at different temperatures (65 °C, 70 °C, and 75 °C) for 4 h. The remaining lipase activity was assayed at 70 °C using olive oil (emulsified in 100 mM Tris-HCl buffer, pH 8.0) as the substrate in a 1:1 ratio for 30 min. Each experiment was conducted three times to obtain the mean value of lipase activity.

Optimal and pH stability

Lipase activity was determined at different pH values by emulsifing olive oil in the following buffers: 100 mM sodium acetate (pH 4.0–6.0), 100 mM potassium phosphate (pH 6.0–8.0), 100 mM Tris-HCl (pH 8.0–9.0), 100 mM glycine-NaOH (pH 9.0–11.0), and 100 mM disodium hydrogen phosphate (pH 11.0–12.0). The reaction was initiated by adding 100 µL of purified enzyme to reaction mixtures containing 2.5 mL of substrate (ratio 1:1 of olive oil and buffer), and the lipase activity was assayed at 70 °C using the method described by Kwon and Rhee (1986).

The pH stability profile of mutant lipase was initiated by mixing 250 µL of purified enzyme in 250 µL of 100 mM Tris-HCl buffer at different pH values (7.0, 8.0, and 9.0) and incubated for 3 h. The residual activity was assayed every 30 min at 70 °C using olive oil (emulsified in 100 mM Tris-HCl buffer, pH 8.0) as the substrate in a 1:1 ratio. Residual lipase activity was measured from the mean values of triplicate assays.

Effect of metal ions

The mutant lipase stability in the presence of metal ions was assessed by pre-incubating the purified enzyme for 30 min at 65 °C with the following metal ions at two concentrations (1 mM and 5 mM): Na^+, K^+, Ca^{2+}, Mn^{2+}, Mg^{2+}, Zn^{2+}, and Fe^{3+}. The control did not contain any metal ions. Lipase activity was assayed at 70 °C using olive oil as the substrate. Relative activities were the means of triplicate assays with ± standard deviations.

Effect of surfactants

The mutant lipase stability was determined by incubating the enzyme with different surfactants. The mixtures were incubated at 65 °C for 30 min in 100 mM Tris-HCl buffer (pH 8.0) containing 0.1% (v/v) or 1% (v/v) of the following surfactants: Tween 20, Tween 40, Tween 60, Tween 80, and Triton X-100. The control did not contain any of these surfactants. The residual activity was measured at 70 °C using olive oil (emulsified in 100 mM Tris-HCl buffer, pH 8.0) as the substrate in a 1:1 ratio. Lipase activities were measured in triplicate and the mean value was taken as the residual activity.

Effect of inhibitors

The effect of inhibitors on the stability of V171S mutant was investigated by pre-incubating the enzyme with 1 mM and 5 mM concentrations of phenylmethylsulphonyl fluoride (PMSF), p-chloromercuricbenzoate (pCMB), and ethylenediaminetetraacetic acid (EDTA) at 65 °C for 30 min in 100 mM Tris-HCl buffer (pH 8.0). Inhibitor-free reaction was regarded as the control (100%) and the remaining activities of the treated enzyme were measured under standard assay condition at 70 °C. All measurements of relative activity were performed in triplicate.

Effect of organic solvents

The effect of organic solvents on lipase activity was investigated by pre-incubating the enzyme with various organic solvents (25% v/v) at 65 °C for 30 min with shaking at 200 rpm. The following solvents were selected to provide a range of log *P* values: methanol (-0.76), ethanol

(-0.24), acetone (-0.23), propanol (0.28), butanol (0.80), propylacetate (1.2), benzene (2.0), heptanol (2.4), octanol (2.9), hexane (3.5), heptane (4.0), isooctane (4.5), dodecane (6.6), and *n*-hexadecane (8.8). Stability was expressed as the residual lipase activity relative to that of the control (without organic solvent). The residual activity was measured at 70 °C using olive oil (emulsified in 100 mM Tris-HCl buffer, pH 8.0) as the substrate in a 1:1 ratio. The mean value of the residual activity was calculated from triplicate assays.

Stability of V171S mutant in different methanol compositions

The effect of methanol on the mutant variant and native lipase Lip 42 was tested with a series of methanol compositions (15, 30, 45, 60, 75, and 90% v/v). The methanol-enzyme mixture was briefly vortexed and pre-incubated at 40 °C with shaking of 200 rpm for 30 min prior to enzyme assay under standard assay condition. The percentage of relative activity was calculated with respect to the highest activity (100%). All samples were conducted in triplicate.

Statistical analysis of the V171S mutant and native lipase

Two-way analysis of variance (ANOVA) was performed with two independent categorical variables, which were the enzyme types (V171S mutant and Lip 42) and methanol compositions (0, 15, 30, 45, 60, 75, and 90% v/v). Post-hoc test was applied to determine which group means differed significantly.

Molecular dynamics simulation of lipases

The structures of Lip 42 (wild-type lipase) and V171S (mutant lipase) were predicted using AlphaFold2 (https://colab.research.google.com/github/sokrypton/ColabFold/blob/main/AlphaFold2.ipynb) (Jumper et al. 2021). The sequence of Lip 42 and V171S lipases was used as an input. Distance Geometry method was used in AlphaFold to generate and construct the protein models. The predicted structures were subjected to verification using online verification tools, including Verify 3D, ERRAT and PROCHECK (https://saves.mbi.ucla.edu/). The 3D models were used to perform molecular dynamics simulations in water and methanol environments using YASARA software package version 12.10.3 (Krieger et al. 2013).

A cubic simulation box was created with a 10 Å buffer distance around all atoms of the protein. Periodic boundary conditions were applied to the protein molecule using the most recent AMBER14 force field in the x, y, and z directions with nonbonded cutoff value of 8 Å. MD simulation was performed in 25% methanol and water at 338.15 K. Before running the simulation, energy minimization was performed using the steepest descent method for approximately 2000 steps, with each sub-step comprising 1.25 femtoseconds across two simulation substeps. MD simulations were performed at 1 bar, 338.15 K for 100 ns after the system reached density equilibration according to the respective solvent relative densities. The molecular dynamics simulation trajectories were further analyzed using built-in modules in YASARA 12.10.3. The stability and flexibility of the simulation trajectories were evaluated by calculating the root mean square deviation (RMSD), radius of gyration, surface accessible area (SASA), and root mean square fluctuation (RMSF) of each residue.

Elastic netwok model-based normal mode analysis

The PDB file of the final simulation snapshots was submitted to the Elastic Network Model (ENM) website (https://www.sciences.univ-nantes.fr/elnemo/) for normal mode analysis (NMA). This online tool is a computational technique used to study the dynamics of macromolecules around their equilibrium conformation and focuses on the low-frequency normal modes, which are critical for understanding large-scale conformational changes in macromolecules. This method simplifies a molecular system by modeling it as a network of nodes connected by bonds or interactions (Suhre and Sanejouand 2004). In this analysis, ENM was employed to compare the mutant and wild-type dynamics in order to understand the contributions of each normal mode to conformational changes.

Principal component analysis and free energy landscape

Principal component analysis and free energy landscape were conducted using GROMACS software (Lindahl et al. 2001). The simulation trajectories from YASARA were converted into trajectory.xtc using md_convert.mcr of YASARA modules. Covariance matrices of lipases in water and methanol were calculated using protein backbone atomic fluctuations following the elimination of rotational and translational motions using the gmx trjconv of the GROMACS tool. The covariance matrices of Ca atoms for the Lip 42 and V171S in water and methanol trajectories were constructed and diagonalized using the gmx covar module of GROMACS software. Gmx anaeig was used to generate the eigenvalues and eigenvectors of the protein backbone atoms. The eigenvectors are directions in conformational space and represent the collective motions of atoms along the directions. The eigenvalues represent the mean square fluctuations (MSF) of atoms along the corresponding eigenvectors. Reaction coordinates, PC1 and PC2 were calculated and concatenated to generate free energy landscape (FEL) of protein using gmx sham to capture the lowest stable energy state. Two- and three-dimensional FEL plots were generated using Matplotlib. Free energy landscape is a useful tool for understanding and analyzing biomolecular

Table 1 Purification enhancement of V171S lipase following affinity chromatography

Fraction	Volume (mL)	Total protein (mg)	Specific activity (U/mg)	Total activity (U)	Yield (%)	Fold purification
Crude	15	32.70	56.42	1845	100	1.0
Affinity chromatography	10	7.12	155.90	1110	60	2.8

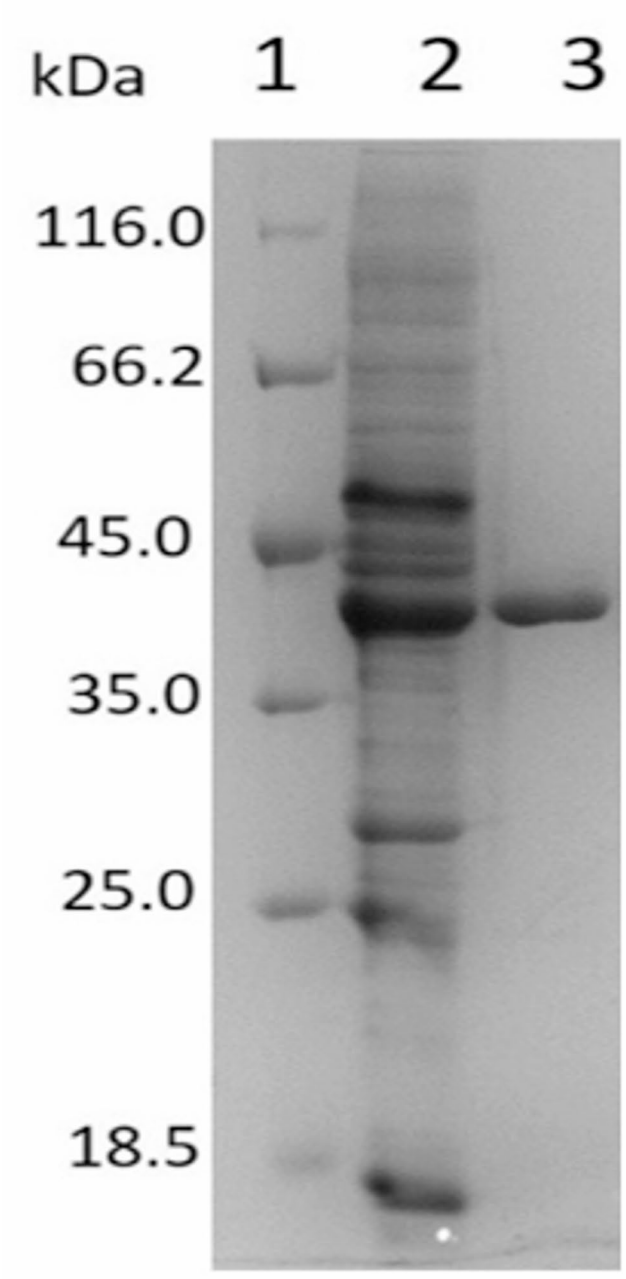

Fig. 1 SDS-PAGE analysis of V171S mutant lipase using Strep-tag II affinity chromatography. Lane 1: Unstained protein ladder expressed in kDa (Fermentas). Lane 2: Crude protein extract. Lane 3: Purified V171S protein at 43 kDa

processes such as protein folding, protein aggregation, and molecular recognition.

Results

Expression and characterization of V171S mutant lipase

The V171S mutant lipase was engineered from Lip 42, originally derived from *Bacillus* sp. strain 42, through a single amino acid substitution in the loop region near the lid, distant from the active site, with the aim of investigating its molecular interactions and conformational behavior in solvent environments. To analyze the effect of Lip 42 mutations on enzyme activity and stability, Strep-tag II affinity chromatography was employed to purify the V171S mutant lipase. As reported in Table 1, the pooled protein fractions contained approximately 7.12 mg of V171S lipase, implying 60% recovery with a 2.8-fold purification factor. The pooled fractions were subjected to SDS-PAGE to determine the protein purity. As shown in Fig. 1, the gel revealed an intense single band with an expected molecular weight of 43 kDa. Using the Strep-tag purification system, excellent purification with good yield of the V17S mutant lipase could be achieved in a single step under mild conditions (Guo et al. 2022).

Characterization of mutant V171S lipase

The effect of temperature on the activity of V171S lipase was determined at various temperature ranges over 30–80 °C at 5 °C intervals. As shown in Fig. 2a, the enzymatic activities of V171S mutant increased steadily with increasing temperatures. The V171S mutant lipase exhibited a slight drop in hydrolysis activity at moderate temperatures from 40 °C to 45 °C, where the enzyme retained 20% of its relative activity. The activity of V171S mutant lipase reached its maximum activity at 70 °C. The activity of V171S lipase decreased sharply at temperatures higher than the optimum temperature, where the mutant retained only 58.8% of relative activity at 75 °C and 39.5% activity at 80 °C.

The thermostability of V171S was determined by measuring the residual enzyme activity after pre-incubation at different temperatures, ranging from 65 °C to 75 °C. Following 30 min of incubation, the mutant lipase exhibited a decline of almost 90% in relative activity at 75 °C, while maintaining 64.3% of its relative activity at the optimum temperature of 70 °C (Fig. 2b). Interestingly, treatment of the enzyme at 65 °C demonstrated great thermal stability, with more than 90% of its relative activity remaining after 30 min of incubation. Within 60 min of incubation at 70 °C, the activity dropped to 47.8% and

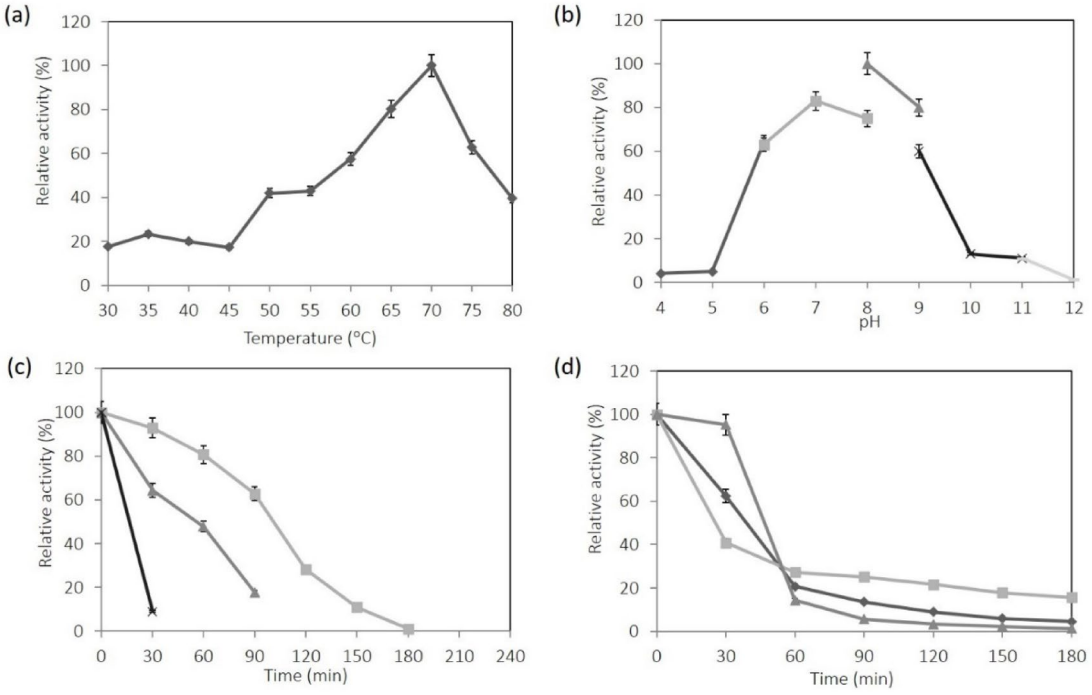

Fig. 2 Characterization of V171S lipase. **a** Effect of temperature on V171S mutant lipase activity. **b** Temperature stability of V171S lipase. The residual activity was measured using olive oil every 30 min at 70 °C. The symbols ■, ▲, and x indicate the temperature of 65, 70, and 75 °C, respectively. **c** Effect of pH on lipase activity. pH buffer system: Sodium acetate buffer (◆); Sodium phosphate buffer (■); Tris-HCl buffer (▲); Glycine-NaOH buffer (x), Na_2HPO_4-NaOH (-). **d** Stability of V171S lipase at different pH environments. The residual activity was measured at 70 °C with the method of Kwon and Rhee (1986) using olive oil emulsified in 100 mM Tris-HCl buffer, pH 8.0) as the substrate in a 1:1 ratio. The symbols ◆, ■, and ▲ indicate pH 7, 8, and 9, respectively. Activities are represented by mean values ± standard deviation of means ($n = 3$)

more than 90% of its relative activity was lost after 90 min of incubation. In contrast, the enzyme maintained 80% relative activity at 65 °C for the same incubation duration and and completely lost its activity after 180 min.

The influence of pH on the activity and stability of V171S mutant lipase was evaluated by measuring the enzyme activity in reaction mixtures with pH values ranging from 4 to 12. The mutant lipase was found to be active over a broad range of pH values from 6 to 9 with maximum activity at pH 8.0, as depicted in Fig. 2c. The maximum catalytic activity appeared to be the same as that of the wild-type Lip 42 at pH 8.0 in 100 mM Tris-HCl buffer. However, under extreme acidic and alkaline conditions, the activity of mutant lipase decreased sharply, falling to 1.0% and 4.5% at pH 4.0 and 5.0, respectively. Treatment under pH 10, 11, and 12 recorded 13%, 11%, and 1.1% of relative activities, respectively.

The pH stability of V171S was examined by measuring the relative enzyme activity after 30 min of pre-incubation in buffer systems ranging from pH 4.0 to 12.0. Based on the obtained results (Fig. 2d), V171S mutant showed good stability at a broad pH range from pH 6 to 9 within 30 min of treatment. Although the optimal pH of V171S lipase was determined at pH 8.0, the enzyme exhibited the highest stability at pH 9.0, indicating that the overall structure of the mutant was more durable at pH 9.0 over time. The remaining activity of V171S mutant declined after 50 min of treatment at all pH values. Overall, the mutant lost 50% of its enzymatic activity after 60 min of treatment at pH 7.0, 8.0, and 9.0.

Metal ion dependency on the activity and stability of V171S mutant was investigated by treating the enzyme with two different concentrations of metal ions (1 mM and 5 mM) for 30 min prior to enzyme assay. As shown in Fig. 3a, the activity of V171S lipase was stimulated by the addition of Ca^{2+}. The addition of 1 and 5 mM Ca^{2+} increased the activity by 33.6% and 23.6%, respectively, relative to the control. In contrast, the addition of Zn^{2+} at 1 or 5 mM inhibited the activity of V171S lipase, reducing the enzymatic activity to 2.2% and 7.7%, respectively. The results obtained were in accordance with the findings on wild-type Lip 42 lipase (Hamid et al. 2009a). Dramatic reductions in the lipase activity of V171S lipase were observed with 1 and 5 mM Fe^{3+}. The activity of V171S lipase was enhanced by 27% in the presence of 1 mM K^+, however, the increase of K^+ to 5 mM reduced the enzyme activity to 41%. A similar trend was observed upon treatment with Mg^{2+} and Mn^{2+}.

Several surfactants were tested for their effects on the lipase activity of V171S mutant lipase at two different

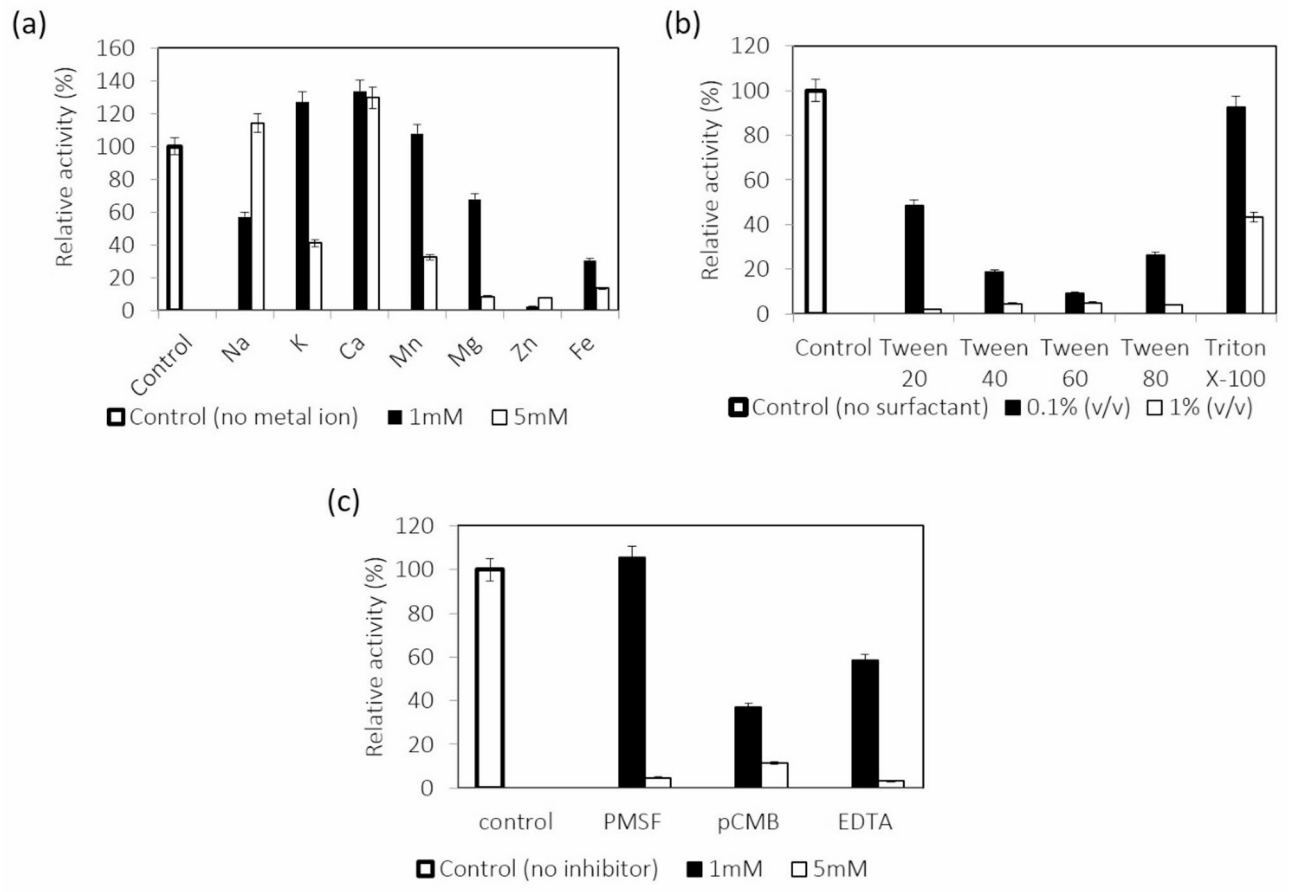

Fig. 3 **a** Effects of metal ions on V171S lipase activity. The residual activity of V171S lipase was determined after incubation with 1 mM or 5 mM of each metal ion at 65 °C for 30 min. **b** Activity of V171S lipase in Tween 20, 40, 60, 80, and Triton X-100. V171S mutant lipase was incubated with 0.1% and 1% (v/v) of each surfactant at 65 °C for 30 min prior to enzyme assay. **c** Influence of inhibitors on the activity of V171S mutant lipase. The enzyme was pre-treated with 1 mM or 5 mM of each inhibitor at 65 °C for 30 min, followed by enzyme assay. The error bar indicates the standard deviations of the mean ($n = 3$)

concentrations (0.1% and 1% v/v). The addition of surfactants did not enhance the overall lipase activity (Fig. 3b). V171S mutant lipase retained 92.7% of its activity in the presence of 0.1% Triton X-100, nevertheless, its activity was greatly reduced by 1% Triton X-100. A negative effect was also observed in the presence of other tested Tween additives (Tween 20, 40, 60, and 80) when the concentration of the additive increased to 1%.

The influence of three different classes of inhibitors, namely PMSF, pCMB, and EDTA, was tested on V171S lipase by measuring the residual activity of the enzyme after 30 min of treatment. High concentration of all inhibitors at 5 mM repressed the residual activity of V171S mutant lipase by up to 80% (Fig. 3c). The presence of 1 mM PMSF increased lipase activity to 105.5%, however, the enzymatic activity was strongly inhibited by the presence of 5 mM PMSF. At 1 mM concentration, pCMB and EDTA inhibited lipase activity by 63.1% and 41.6%, respectively and stronger inhibition was observed when the enzyme was exposed to higher inhibitor concentrations.

The effect of organic solvents with different polarity index, ranging from − 0.76 to 8.8 on V171S lipase stability was analyzed at 65 °C. V171S mutant lipase demonstrated notable stability across tested organic solvents with log P ranging from 0 to 3, with the exception of propyl acetate, maintaining over 60% of its relative activity after 30 min of incubation (Table 2). Upon exposure to heptanol, the V171S mutant lipase exhibited an increase in activity, retaining 106.8% of its initial activity. The mutant retained high activity in the presence of acetone with 95.7% of residual activity, followed by ethanol with 94.7% of activity was remained. A similar observation was found when exposed to 1-propanol, where the enzyme showed marked tolerance, retaining 91.9% of its activity. The addition of methanol maintained the original activity by 71.9%. The lowest relative activity retained was observed when the enzyme was exposed to propyl acetate with only 28.4% of activity. High residual activity was recorded when treated with hydrophobic solvents (Log $P > 2$), where 93.6% and 82.3% of relative activities

Table 2 Organic solvent stability profile of V171S lipase

Organic solvents	Log *P*	Relative activity (% ± SD)
Control	-	100
Methanol	-0.76	71.9
Ethanol	-0.24	94.7
Acetone	-0.23	95.7
1-Propanol	0.28	91.9
Butanol	0.80	72.6
Propyl acetate	1.2	28.4
Benzene	2.0	64.8
Heptanol	2.4	106.8
Octanol	2.9	86.1
Hexane	3.5	83.3
Heptane	4.0	71.4
Isooctane	4.5	74.1
Dodecane	6.6	93.6
Hexadecane	8.8	82.3

were retained when treated with dodecane and hexadecane, respectively.

Mutation effect on methanol stability

The effect of mutation on the stability of Lip 42 lipase in methanol was investigated by conducting a comparative study with the mutant upon treatment with different methanol compositions. As shown in Fig. 4, the methanol stability profile demonstrated that the V171S mutant exhibited markedly improved tolerance to methanol compared to the native Lip 42 lipase, particularly at low to moderate concentrations (15–45% v/v). The highest relative activity of V171S mutant was observed at methanol concentration of 45% v/v. However, at higher methanol concentrations of above ≥ 60% v/v, both the native and mutant enzymes experienced a dramatic decline in activity.

Statistical evaluation of the methanol stability study

From the experimental results at 40 °C pre-incubation of enzyme–methanol mixtures, the residual activity differences between the native Lip 42 and the V171S mutant were relatively small at higher methanol concentrations. However, post-hoc analysis using the Tukey HSD test showed that Lip 42 differed significantly from the mutant with *p*-values less than 0.05 (Table 3). This finding provides strong evidence against the null hypothesis, indicating that the observed differences were statistically significant. Although the confidence intervals (CIs) were relatively wide due to the limited number of replicates, the reported 95% CIs were still consistent within the range that supported the *p*-values.

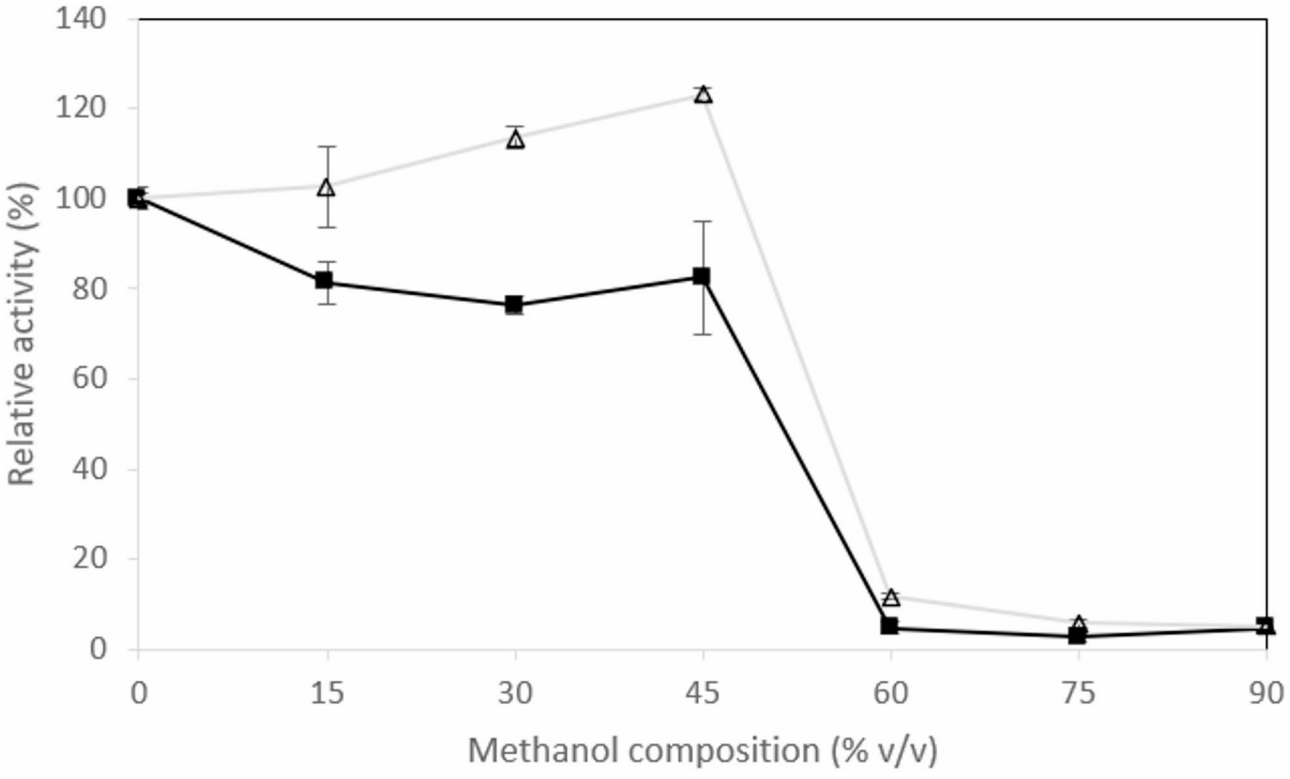

Fig. 4 Methanol stability profile of V171S mutant and Lip 42 lipase. The enzymes were pre-incubated in different methanol compositions at 40 °C. The symbols ■ and Δ indicate native lipase and mutant, respectively. The error bar represents the standard deviations of mean ($n = 3$)

Table 3 Statistical analysis of variance (ANOVA) for lip 42 and V171S mutant

					95% Confidence Interval		
(I)	**(J)**	**Mean difference (I-J)**	**Std. error**	**Sig.**	**Lower bound**	**Upper bound**	**Significance $P < 0.05$**
Lip 42	V171S mutant	-23.5976	6.01279	0.001	-38.2056	-8.9895	Yes

Table 4 Quality assessment of lip 42 and V171S lipases

Analyses	Lip 42	V171S
Verify 3D	97.4%	98.2%
ERRAT	93.9%	94.2%
Ramachandran Plot		
Residues in most favored regions	90.9%	92.4%
Residues in additional allowed regions	8.8%	6.9%
Residues in generously allowed regions	0.3%	0.6%
Residues in disallowed regions	0.0%	0.0%

Molecular dynamics simulation of lipases in methanol

The three-dimensional structure was developed using AlphaFold2, the latest technology in protein model structure development. To ascertain the stereochemical integrity of the constructed structure, various parameters such as bond lengths, bond angles, torsion angles, and amino acid chirality were examined using structure validation tools, including Verify 3D, ERRAT, and PROCHECK. The 3D structures of Lip 42 and V171S passed the Verify 3D test with scores of 97.4% and 98.2%, respectively, which indicates the score of a satisfactory predicted model. ERRAT analysis yielded a quality factor of 93.9% for Lip 42, whereas V171S 3D model produced a scoring of 94.2%, which fell below the 95% rejection limit. However, ERRAT score of above 80% was still acceptable and the 3D models were considered to pass this verification. The Ramachandran plot analysis of the predicted Lip 42 and V171S lipase structures revealed that approximately 90.9% and 92.4% of the residues occupied the most-favored regions, respectively (Table 4). Meanwhile, 8.8% and 6.9% of residues were found in the regions that were additionally allowed for Lip 42 and V171S lipases. In both structures, no residues were located in the disallowed regions. Hence, the 3D models of Lip 42 and mutant V171S can be reckoned as good-resolution structures.

Among the various solvents tested experimentally, methanol was selected as the solvent system for detailed kinetic simulations because of its direct relevance for biodiesel production, where lipase catalyzes the transesterification reactions between triglycerides and methanol. The structural dynamics of Lip 42 and V171S lipases were investigated under aqueous and methanol environments by molecular dynamics simulation trajectories at 65 °C over 100 ns. From Fig. 5a, the RMSD profile for wild-type Lip 42 and V171S mutant in water environment exhibited only minor fluctuations and remained stable over the course of simulation with RMSD value below 2 Å which closely aligned with the starting structure. Notably, Lip 42 simulated in methanol exhibited large fluctuation across 100 ns trajectories with RMSD score of average 1.5 Å. In contrast, V171S mutant in methanol displayed an average RMSD at around 1.5 Å to 2 Å with minimal fluctuations across 100 ns.

Radius of gyration analysis revealed that lipases Lip 42 and V171S maintained their compactness and folded structure in water throughout 100 ns of simulation, reflected by a small degree of fluctuations (Fig. 5b). Rg profile for Lip 42 lipase in methanol displayed multiple fluctuations throughout the simulation. In the case of V171S mutant, the Rg trend fluctuated in the first 70 ns of simulation and became constant toward the end of the trajectories. Solvent accessible surface area (SASA) analysis serves to evaluate the extent of solvent exposure, providing insights into protein stability, folding, and solvent interactions. From Fig. 5c, Lip 42 in water displayed the lowest SASA value of around 15,500 Å with smooth fluctuations. A similar profile was observed for V171S mutant with a consistent SASA score throughout the trajectories. In a solvent-rich environment, both lipases displayed high SASA values. Lip 42 exhibited several fluctuations over the course of the 100 ns trajectories. At the beginning of the simulation, small fluctuations in the SASA value were observed for the mutant lipase and started to increase at 30 ns. However, the SASA trend became constant towards the end of the simulation.

The flexibility of each residue can be assessed by analyzing the RMSF values during the simulation. The results highlighted a notable increase in atomic mobility in the lid area for Lip 42 and V171S mutant in aqueous system, as depicted in the red box of Fig. 6a. In aqueous conditions, both wild-type and mutant showed high RMSF values at lid 1 with residue index window of 170 and 196, and lid 2 area with residues from 209 to 235, indicating inherent flexibility. In methanol environment, the V171S variant demonstrated an increase in fluctuation in the region from Arg21 to Gly31, which corresponded to the loop region. In the mutant, Lid 2 region exhibited reduced fluctuation compared to the wild-type, while Lid 1 showed increased mobility. The decreased fluctuation of Lid 2 likely contributes to greater structural rigidity, which can protect the enzyme from solvent-induced destabilization.

Figure 6b and c show simulation snapshots of comparative flexibility at 0 ns and endpoints of both wild-type and mutant conformations in water and methanol systems. From the structural overlay of wild type Lip 42, a slight deviation in lid 1 and lid 2 positions after 100 ns in methanol (yellow) compared to the starting structure

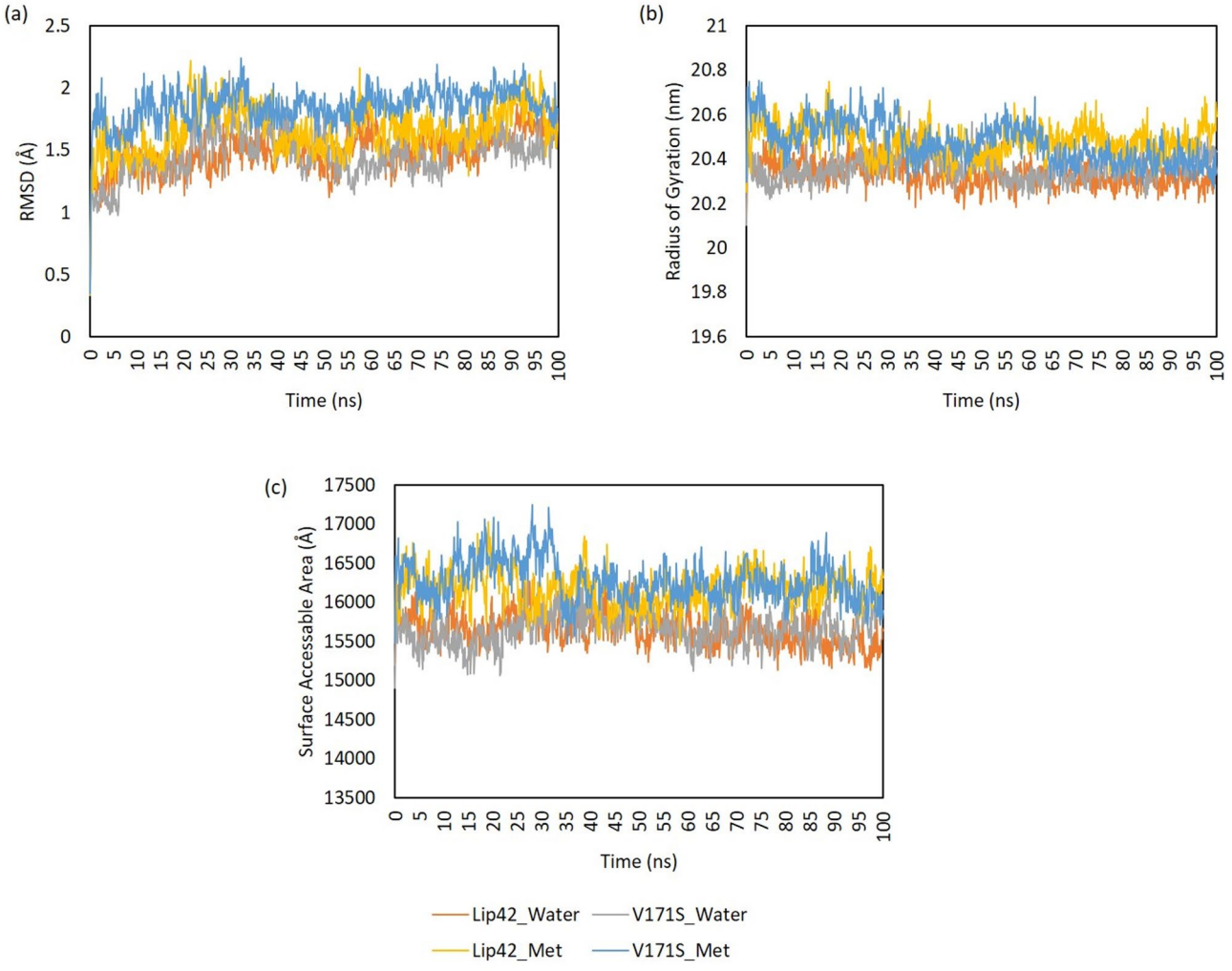

Fig. 5 Molecular dynamics simulation analysis of Lip 42 and V171S in water and methanol. **a** Root mean square deviation of Lip 42 and V171S lipases. **b** Radius of gyration of Lip 42 and V171S lipases. **c** Surface accessible area of Lip 42 and V171S lipases

(grey) and water simulation (blue) was observed. Meanwhile, for the mutant, the Lid 1 region remained fairly close to the starting conformation. Active site residues (Ser113, Asp317, and His358) for both lipases in two different systems remained structurally conserved, although slight shifts were visible.

Normal mode analysis

Figure 7 shows the disturbance of motion or state of equilibrium for Lip 42 and V171S lipase structures in both water and methanol systems. The perturbed structures from the NMA analysis were superimposed with the initial structures at 0 ns to illustrate the lid opening motions of Lip 42 and V171S in water and methanol. From Fig. 7a and c, the normal mode analysis revealed that V171S mutant in water showed more ordered and compact motion compared to the wild type between 0 ns and 100 ns. While the NMA snapshots of V171S in methanol showed some local motions at Lid 1 and Lid 2 (Fig. 7d), the movements were more localized rather than widespread. The zoom-in views indicated moderate and coordinated shifts of the lid regions, which likely contributed to the mutant enhanced adaptability at high temperatures in the methanol environment.

Principal component and free energy landscape analyses

PCA has been widely used to reduce the complexity of MD data while preserving most of the data variation. In this study, PCA was performed to study the major conformational transitions of Lip42_water, Lip42_met, V171S_water, and V171S_met from the MD simulation trajectories. Two-dimensional projections of PC1 and PC2 between the two largest eigenvalues in each system were mapped in Fig. 8a. The conformation of each lipase system over the trajectories of 100 ns was represented by dots. In this analysis, Lip 42 lipase in methanol

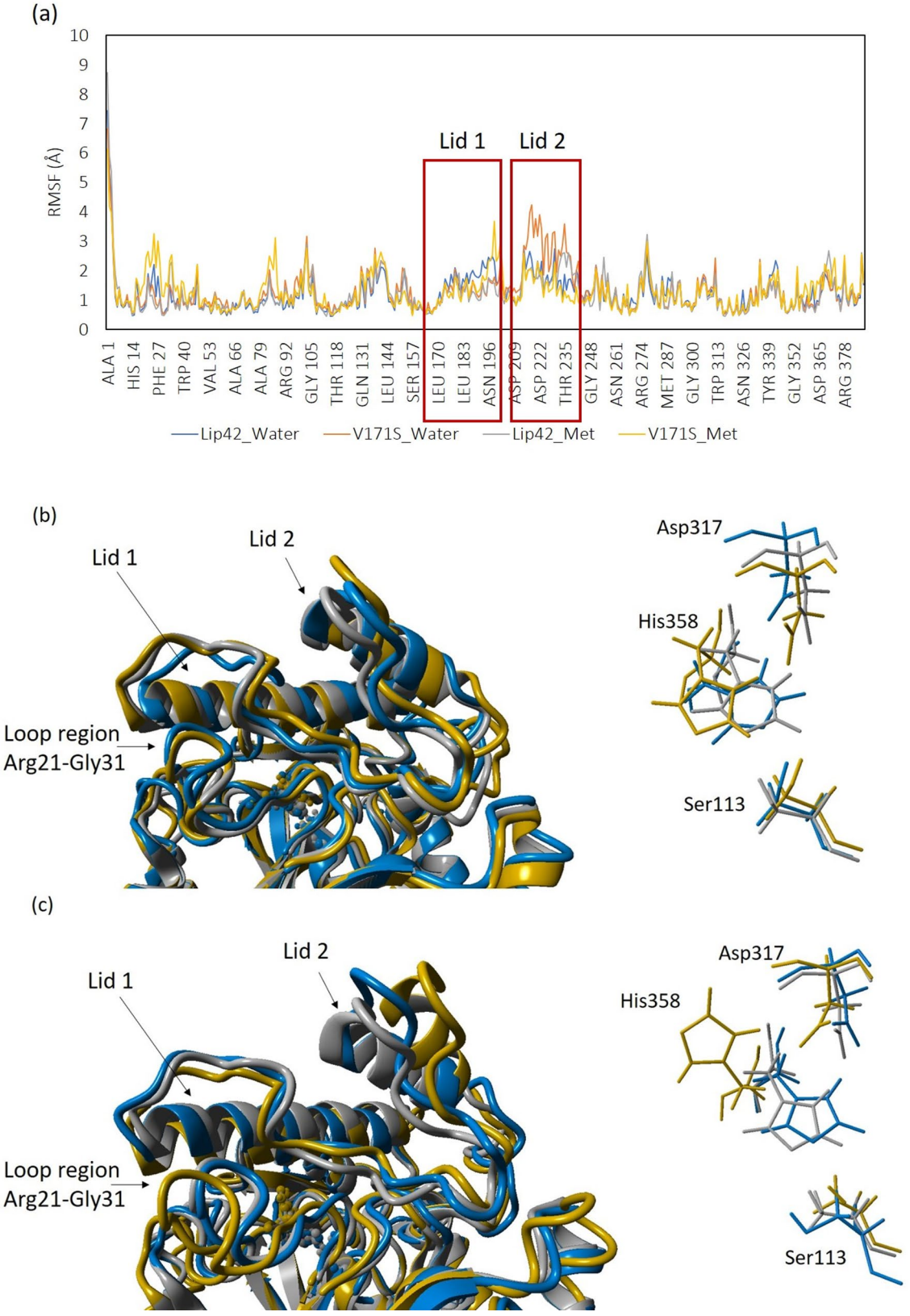

Fig. 6 Lipase fluctuation and structural changes during simulation **a** Root mean square fluctuation of Lip 42 and V171S residues for 100 ns of simulation in water and methanol. **b** Wild-type lipase before and after simulation in water and methanol. **c** V171S mutant lipase before and after simulation in water and methanol. Colour represents the starting lipase structure at 0 ns (grey), the lipase structure after 100 ns in water (blue), and the conformation after 100 ns in methanol (yellow). The active site residues consisting of Ser113, Asp317, and His358 were presented in the stick

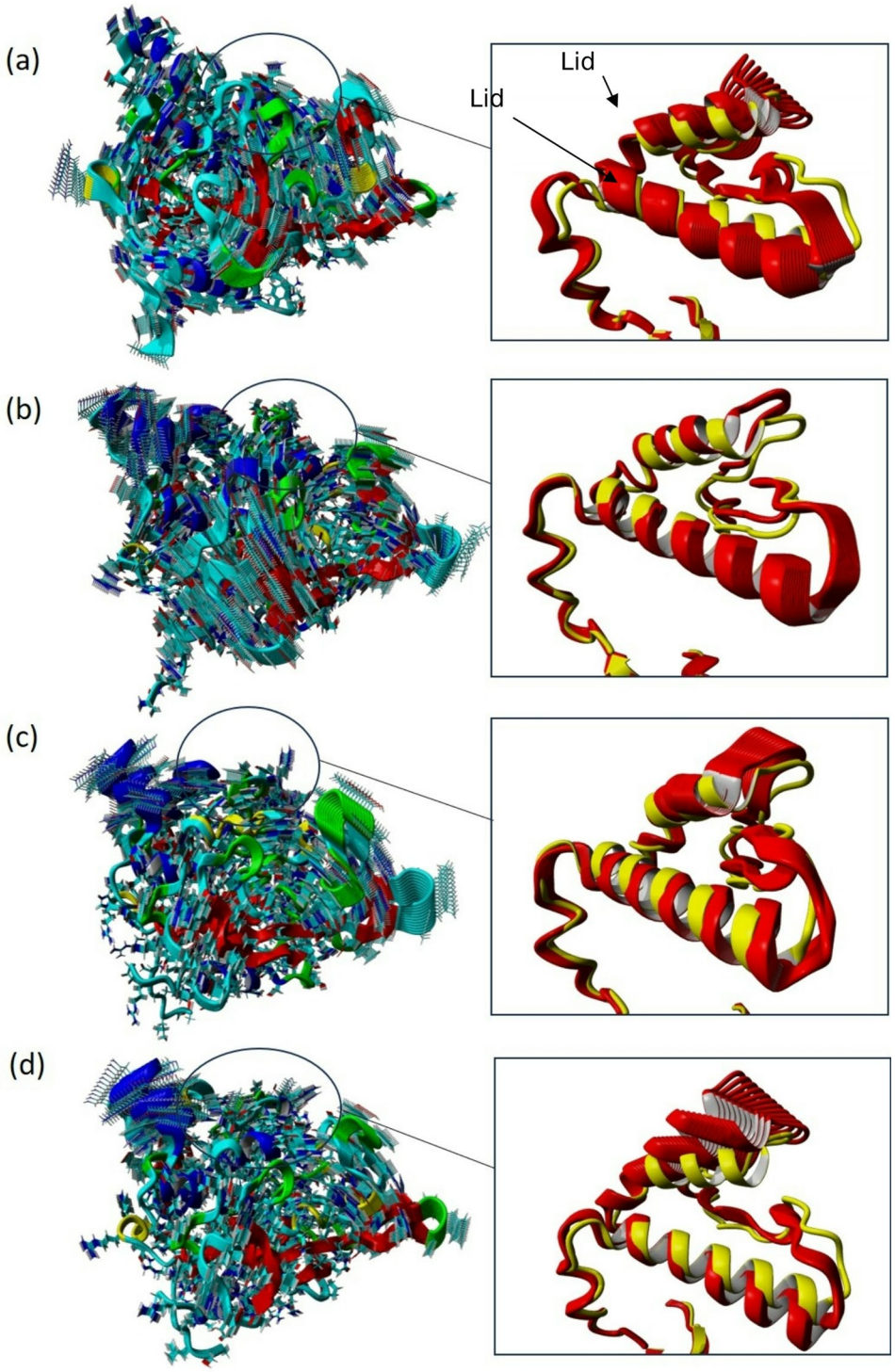

Fig. 7 Normal mode analysis of Lip 42 and V171S in water and 25% methanol. **a** Lip 42 in water. **b** Lip 42 in methanol. **c** V171S in water. **d** V171S in methanol. The right panel shows a close-up view of the superimposed NMA cluster (red) with respect to the initial structure at 0 ns (yellow). The long α-helix corresponds to Lid 1, while the shorter α-helix corresponds to Lid 2

was scattered over a large area, showing a dispersed type of motion on the first two components, PC1 and PC2. The V171S mutant exhibited more PCA spread clusters, especially toward the edge. In addition, eigenvalues were plotted against the eigenvector to show the magnitude of motion along each principal component (Fig. 8b). Lip42_methanol exhibited the largest amplitude motions, which were reflected from the first few eigenvalues.

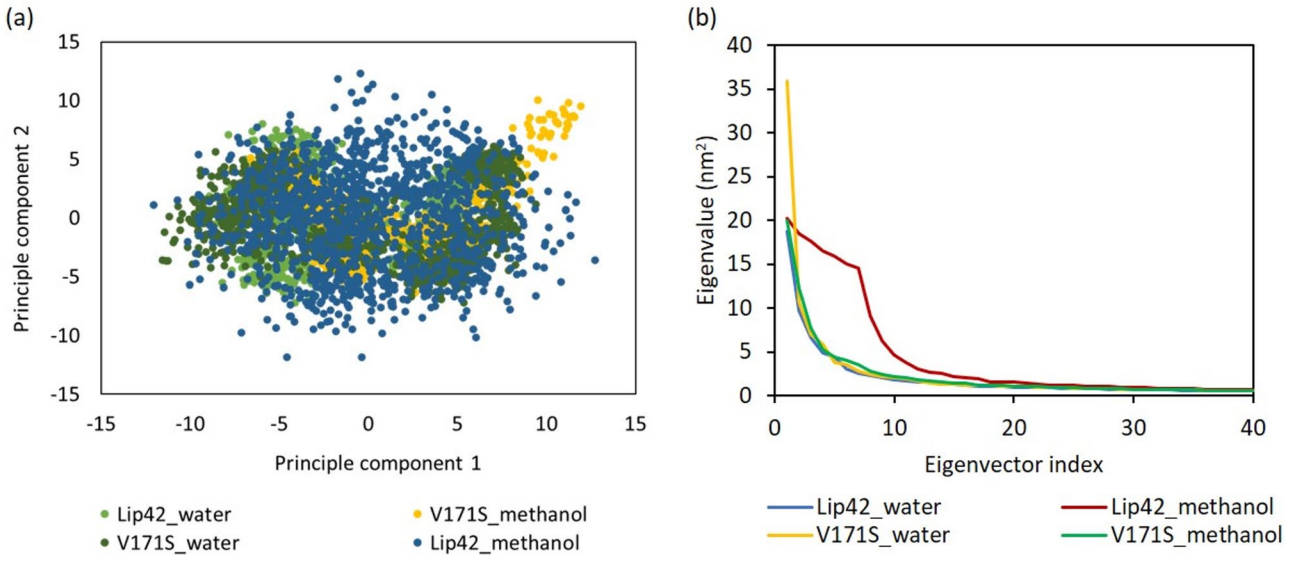

Fig. 8 Essential dynamics analysis. **a** Principal component analysis of wild-type Lip 42 and mutant (V171S) in water and methanol. **b** Eigenvalues for lipase models as a function of the eigenvector. The plot shows the eigenvalues for the first 40 eigenvectors

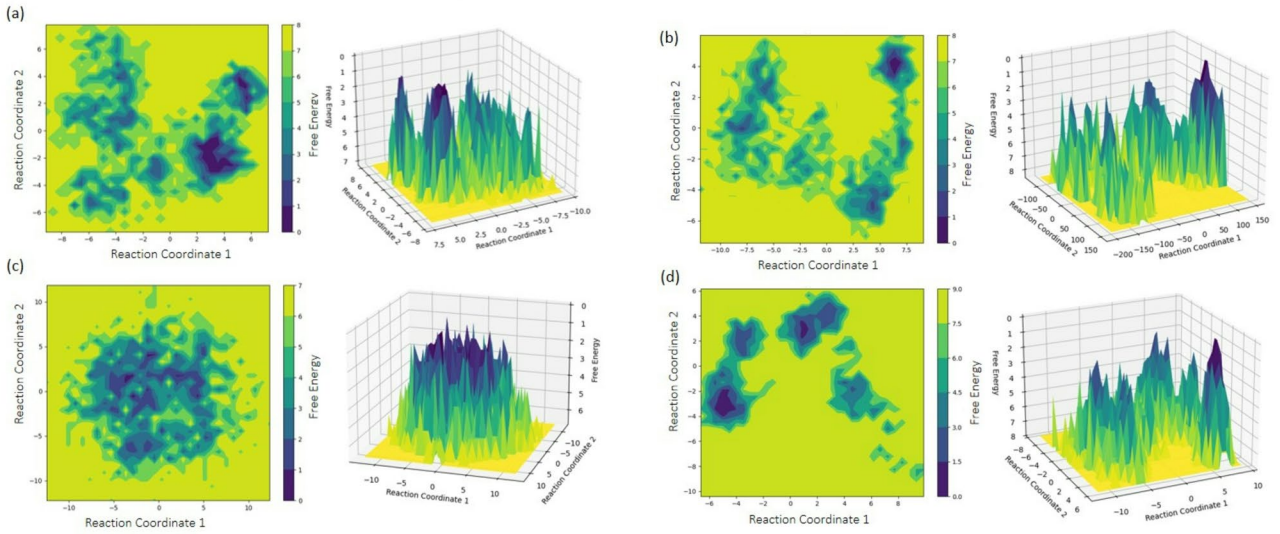

Fig. 9 Free energy landscape (FEL) contour plots of lipase in water and methanol systems. **a** Lip 42 (wild-type) in water. **b** V171S lipase in water. **c** Lip 42 (wild-type) in methanol. **d** V171S lipase in methanol. The first panel represents the two-dimensional FELs of lipase and the second panel represents the three-dimensional FEL landscape. The lowest energy clusters in all systems are shown by dark blue. The high energy state is represented by a yellow color in the plot

V171S_methanol displayed reduced large-scale fluctuations with lower eigenvalues.

Free energy landscape analysis was conducted to identify the stable states and conformational transitions of lipases based on essential dynamics. The two- and three-dimensional structures of free energy landscape contour maps for the lipase systems were obtained from PC1 and PC2 and represented in Fig. 9. The contour maps of Lip 42 in the water system revealed scattered multiple small dark blue regions and some broad areas of intermediate energy (Fig. 9a). From 3D FEL, Lip42_water showed stable conformational states, reflected by moderate rugged landscape with multiple peaks and valleys, which represents energy barriers. V171S in water was more stable and less dynamic than wild-type in aqueous conditions with smoother energy landscape, as observed in Fig. 9b. V171S_methanol showed a clear global energy minima basin (blue color), whereas Lip 42 revealed several basins with dispersed energy minima states. From Fig. 9c, the free energy landscape showed a highly scattered

and noisy distribution of free energy basins covering a large area. The corresponding 3D FEL was rugged with many narrow energy peaks and high-energy regions. The energy cluster in V171S in methanol systems was observed to be less scattered, indicating the robust and stable interactions of V171S (Fig. 9d). The 2D FEL displayed distinct, well-defined low-energy basins, and the 3D surface was smoother with fewer valleys.

Discussion

In this study, V171S mutant lipase was subjected to biochemical characterization with various parameters to fully understand how the mutation impacts enzyme stability, activity, and industrial applicability. Thermal stability is one of the key determinants of whether an enzyme is practically useful and economically viable. The variant exhibited similar maximal activity at 70 °C to the wild-type lipase, Lip 42. This indicates that the mutation did not affect the catalytic performance and structural conformation of lipase related to temperature-dependent activity. Accordingly, V171S mutant lipase was considered a thermostable lipase. V171S mutant remained relatively stable for at least 105 min at 65 °C without major loss of activity. These findings indicate that the mutant thermostability is on par with the wild-type Lip 42 (Hamid et al. 2009a). The notable thermal tolerance of the V171S variant highlights its potential for application in thermally demanding industrial settings such as biofuel production. In a previous report, the mutant *Bacillus cereus* EV4 showed thermostable properties with maximal activity at 60 °C (Irianto et al. 2024). Deviations from the ideal pH range can significantly impact enzyme activity and stability. Therefore, determining the pH for an enzyme to function optimally is crucial. Mutant lipase stability in a broad pH environment ranging from pH 6.0 to 9.0 suggests that the enzyme is compatible with process fluctuations and pH shifts during a reaction. The optimum pH value indicates that V171S mutant is an alkaline lipase. This finding is consistent with other studies on *Bacillus* lipase, as shown by the lipase of *Bacillus licheniformis*, which has optimum activity at pH 8.0 (Zhao et al. 2021).

Previous report showed that the wild-type Lip 42 lipase contains a zinc-binding region. No increase in activity was observed upon addition of Zn^{2+}, suggesting that the enzyme does not require zinc as a catalytic cofactor. Although metal ions tested were beneficial at low concentrations, the mutant enzyme had lower tolerance at high concentrations, possibly due to structural changes caused by the mutation. Ishak et al. (2019) proposed that the presence of calcium ions affects the catalytic behavior of lipase by improving the binding of 5 M lipase to the substrate. Calcium ions enhanced the activity of V171S lipase by 38%. This behavior toward calcium was comparable to that of wild-type lipase and lipases from *Bacillus licheniformis* NCU CS-5, with enzyme activity increasing to 156.17% in the presence of 10 mM Ca^{2+} (Zhao et al. 2021). Zhang et al. (2020) demonstrated that calcium ions improve substrate-binding and catalytic efficiency. The findings suggest that the enzyme appears to be metal-activated, especially by divalent cations such as Ca^{2+} and Mg^{2+}, rather than being strictly metal-dependent.

The behavior of V171S lipase in the presence of surfactants is consistent to the previous findings of *Aspergillus niger* lipase in which the enzymatic activity decreased in the presence of high concentrations of Triton X-100 (Xing et al. 2021). In contrast, another study found that treating lipase with Triton X-100 at 5% and 10% concentrations considerably increased activity to 123% and 128%, respectively (Abol-Fotouh et al. 2021). This result is similar with a previous report in which lipase activity of *A. oryzae* was suppressed to almost 80% by Tween 20 and Tween 80 (Paitaid et al. 2021).

V171S lipase was strongly inhibited by PMSF even at low concentration. PMSF is an irreversible serine inhibitor that inactivate enzyme permanently (García-Carreño 1992). Amalia et al. (2020) proposed that the depletion of enzyme activity in the presence of an inhibitor may be due to the modification of the active site, which prevents the enzyme from interacting with the substrate. Low PMSF concentration may bind to non-catalytic serine and cause conformational stabilization, whereas high PMSF concentration forms a covalent bond with active serine that blocks catalytic function. This result confirms the involvement of a serine residue in the active site, indicating that the mutation did not disrupt the accessibility of catalytic serine and that the mechanism of catalysis is unchanged. Strong inhibition by the thiol inhibitor pCMB to the catalytic activity of V171S mutant lipase revealed an important role for the SH group in the catalytic mechanism. The enzyme exhibited metal-ion facilitation at optimal concentrations, but was not strictly metal-dependent. EDTA sensitivity at high levels showed some reliance on the activation of divalent ions, which is in line with the findings in the previous section. A similar inhibition by EDTA and pCMB was also observed on lipase from *Bacillus coagulans* (Al-Ghanayem 2021).

Organic solvents play an important role in many industrial processes involving enzymes, particularly in chemical and biochemical reactions (Chemat et al. 2019). Interestingly, the mutation of Lip 42 lipase displayed high tolerance toward both polar and hydrophobic solvents under temperature stress. Previous findings recorded low residual activities of wild-type Lip 42 lipase when exposed to solvents with log *P* values of 4 and above. While lipase Lip 42 tolerated methanol at moderate temperatures, its stability deteriorated when exposed to

methanol at elevated temperatures (Hamid et al. 2009a). The V171S variant, however, maintained high catalytic activity following treatment with 25% v/v methanol at 65 °C. The stability enhancement in water-miscible solvents suggests that the V171S mutant lipase has greater potential for industrial applications such as biodiesel production, particularly under harsh processing conditions. Previously, the structure-based rational design method was applied to develop a Ser16Gly lipase mutant of *Bacillus subtilis*. The mutant lipase improved ethanol stability compared to the wild-type (Min et al. 2021). Enzymatic activity enhancement in the presence of organic solvent was also reported on A83D/K251E, A83D/M121I/K251E/G327S and A83D/M121I/S195N/T272M mutants from *Geobacillus zalihae* T1 lipase (Maiangwa et al. 2021).

According to stability profile with a series of different methanol concentrations, the V171S mutant showed a higher tolerance of methanol compared to Lip 42 lipase, especially at low to moderate concentrations. While the native lipase gradually lost activity in this range, the mutant not only retained full activity but also displayed enhanced catalytic performance, suggesting that the V171S substitution may stabilize the enzyme structure. However, detrimental effects on the relative activities of both enzymes were observed at high methanol concentrations, which indicated that excessive methanol disrupted protein folding and denatured the enzymes regardless of the mutation. Statistical analysis using one-way ANOVA followed by Tukey post-hoc test revealed a significant difference in residual activity between the native Lip 42 and the V171S mutant after pre-incubation with methanol at 40 °C. The V171S mutant showed a mean activity that was 23.6% higher than that of the native enzyme ($p = 0.001$). The 95% confidence interval (–38.21 to – 8.99) excluded zero, confirming that the observed difference was not due to random variation. This finding indicates that the substitution at position 171 (Val to Ser) enhanced the enzyme tolerance towards methanol. Specifically, Ser171 formed two hydrogen bonds with Thr168 at distances of 2.35 Å and 1.77 Å, respectively. These additional hydrogen bonds likely introduce new stabilizing interactions in the loop region near the lid and strengthen the local structural network, thereby enhancing the overall stability of the enzyme in organic solvents.

To elucidate the structural basis of V171S mutant stability, in silico methods including molecular dynamic simulations, normal mode, and free energy landscape analysis were applied to analyze its structural dynamics and conformational behavior. RMSD analysis was used to quantify the average deviations in atomic positions over time, comparing the simulated conformation with an initial structure as a reference. The structural dynamic of the variant was compared with that of the wild-type lipase at 65 °C in aqueous and methanol environments over 100 ns trajectories. From the RMSD profile, both wild-type and variant lipases exhibited minor fluctuations throughout the simulation course with low RMSD score. This indicates that the atomic proteins of both lipases did not significantly deviate from the native conformations in water environment. In methanol conditions, it was found that the RMSD score for the variant exhibited minor fluctuations at the beginning of the simulation and became constant towards the end of the trajectories despite having a higher RMSD score than the wild-type lipase. A high RMSD value does not inherently indicate structural instability, rather, the consistency and low fluctuation of the trajectory over time are more indicative of conformational stability (Martinez 2015). The wild-type lipase showed greater fluctuations throughout the simulation, indicating lower conformational stability. The mutant lipase exhibited a slightly higher average deviation (2.0 Å) compared to the wild-type (1.5 Å), where the mutant lipase overall trajectory was more stable and consistent. The result suggests that the mutant has better structural adaptation in 25% methanol, which correlates with the enhancement of enzymatic activity observed experimentally. According to Shehata et al. (2020), stabilized RMSD data showed an equilibrium of protein conformation throughout the simulation course, as demonstrated in their study of the open and closed structure of *Bacillus thermocatenulatus* lipase (BTL2).

The radius of gyration (Rg) is a key structural parameter used to evaluate the compactness and folding state of a protein during molecular dynamics (MD) simulations. A smaller Rg value indicates a more compact and tightly folded protein structure, whereas a larger Rg value suggests a more expanded and unfolded conformation. Constant low Rg value with small fluctuations of V171S variant towards the end of trajectories indicates that the mutant became more compact and retained the native-like folded structure. The mutant displayed enhanced structural stability in methanol by adopting a tighter structure to protect the active site and increased resistance to denaturation, which correlates with higher functional retention in solvent-rich environments. SASA analysis revealed a similar pattern, with the mutant exhibiting lower SASA at the end of simulation period. This suggests that less solvent exposure and greater hydrophobic core shielding were adopted to maintain the proper structure.

The RMSF values of the protein backbone Cα atoms were measured to track the fluctuation of each residue throughout the simulation. The mutant displayed higher fluctuation than the wild-type in the lid 1 region of around 4 Å. Although Ser171 is located on a loop near the lid and distant from the catalytic triad, the substitution

appears to modulate lid dynamics indirectly. Enhanced flexibility in Lid 1 may facilitate substrate access and product release by promoting the transient opening of the active site, while the reduced mobility of Lid 2 likely contributes to structural stability and protection against solvent-induced unfolding. Lipases often have flexible lid domains that control access to the active site. Hence, high RMSF in these regions is expected, especially in solvent-exposed and high-temperature environments. Interestingly, structural visualization showed a minor shift in the position of the catalytic His358 residue, suggesting a stable but slightly altered conformation. Rather than being detrimental, this subtle change may reflect an adaptive repositioning that supports the enzyme functionality in a methanol-rich environment. RMSF represents the time-averaged positional fluctuations of residues over the entire trajectory, whereas snapshots capture only instantaneous conformations. Integration of the RMSF result and visual inspection of V171S mutant at the lid 2 region suggests a gradual, stable transition, not random fluctuation. In general, V171S mutant has the capability to preserve structural integrity in methanol environments.

Protein function is closely related to its motion. To determine the effects of mutations on the internal mechanics of protein conformations, the final pdb structures at 100 ns of each simulation were subjected to NMA analysis to investigate the flexibility and motion of lipases. The Elastic Network Model conducted on Lip 42 and V171S lipases in water and methanol systems revealed that the predicted collective motions correlated with the conformational changes of lipases. This motion suggests that the mutant retained moderate flexibility in aqueous condition possibly due to altered local interactions. The superimposition suggests that the mutant retained its structural integrity better in methanol. Ong et al. (2023) reported a similar finding, that high concentrations of methanol and ethanol induced moderate lid opening in mutant lipase during simulations in methanol systems. In methanol systems, moderate lid opening can mimic interfacial conditions and maintain enzyme activity in non-aqueous media, which is important in biodiesel production. A normal mode analysis was conducted by Noby et al. (2021) to confirm the flexibility and cap region of cold-active esterase, demonstrating that a significant amplitude of flexible motion was achievable while maintaining its bonding and steric geometry. Similar to our findings, conformational variation was observed in the lid regions, especially in the second lid. The second lid (residues 220–230) deviation was more flexible and had a higher in fluctuation profile compared to the first lid (residues 175–197) for both lipases in methanol systems. Noby et al. (2021) also compared the flexibility of cold active esterase from *Bacillus cohnii* (EstN7) with its closest homolog, a putative heroin esterase from *Rhodococcu*s sp. (HerE), and demonstrated that the addition of a single amino acid in the loop region induced flexibility in the structure of HerE at the specific region, resulting in higher B-factors.

Notably, if a protein showed large conformational changes, the distribution was broad and scattered in the conformational space, indicating a stable alternate conformation. The first few eigenvectors capture the most significant movements. Both of the lipases showed low overall variance in water system, indicating more compact and stable motion. Overall, the scattered PCA combined with high eigenvalues showed a possibly unstable Lip 42 lipase in the methanol environment. V171S_methanol displayed less structural distribution compared to Lip42_methanol. Hence, it can be concluded that V171S was more stable in the methanol system. Free energy landscape describes the conformational motions of a protein through a very high-dimensional space. The result suggests that V171S mutant had a more stable cluster compared to the Lip 42. This implies that the mutant lipase adopted fewer conformations which help in maintaining the protein core stability under methanol-induced stress.

Khan et al. (2020) reported that a more stable wild-type showed a lower energy state in the free energy landscape plot compared to the mutant, which showed dispersion in a high energy state on the FEL plot. Basith et al. (2021) suggested that a single cluster of energy minimum represents a robust and stable interaction as observed in the agonist-bound glutamate dehydrogenase (GDH). The two related basins separated by a medium barrier suggest an easy transition between two metastable structures. The presence of two medium basins with low energy clusters on FEL of V171 mutant in methanol indicates the existence of an important metastable conformation population. This study demonstrated how mutation directly affects the flexibility of the conformation. In another study, the mutation of the R29S mutant created an impact on flexibility and rigidity, leading to the formation of several basins with distinct low-energy minima that may indicate various metastable conformations. Drici (2023) concluded that the local water network creates a stable environment around the polar hydroxyl group (OH) of the serine residue that is displayed by the mutation of R29S, presented by two closely spaced deep basins to a near native condition. Similar to this study, the deeper and wider native state basins displayed in the 2D plots indicate that the mutation of the non-polar valine residue on Lip 42 lipase to polar serine may help to mimic water-like interactions, even in a methanol-rich environment. This finding concludes that a single mutation in the lid area can appropriately preserve the native-like architecture and enhance the overall conformational structure. This observation aligns with earlier PCA and

NMA findings, where V171S demonstrated more compact and stable dynamics, underscoring its potential as a solvent-tolerant variant suitable for industrial applications in non-aqueous environments. The improvement observed in the V171S mutant highlights the role of the lid domain in regulating lipase stability and solvent tolerance. Specifically, substitution with a smaller, polar residue (Ser) at position 171 appears to modulate the local flexibility and solvent interactions, enabling the enzyme to maintain higher activity in methanol. Therefore, such modification may serve as a reference strategy for engineering other lipases with improved tolerance to organic solvents. Nonetheless, the extent of regularity will likely vary depending on the lipase family, structural fold, and solvent system, underscoring the need for further comparative studies across different enzymes.

Conclusion

High temperature condition offers several benefits in enzymatic biodiesel production, where efficiency and reaction speed are important. This study highlights the impact of V171S mutation in methanol-rich environments at high temperature on the structural dynamics and stability. Functional characterization revealed optimum conditions of V171S mutant at pH 8.0 and 70 °C, and relatively stable at 65 °C. Notably, V171S mutant lipase exhibited an excellent improvement in methanol tolerance at high temperature compared to the wild-type lipase. According to the MD analysis, the balance of flexibility and rigidity of the lid regions served as a viable strategy to maintain enzyme function. The mutation reduces conformational fluctuations as shown by NMA and PCA, and confines the enzyme to stable conformations. These findings demonstrate that targeted single-point mutagenesis of V171S can improve solvent tolerance. This study not only enhances our understanding of structure-function relationships under solvent stress but also provides a foundation for designing more resilient enzymes for industrial biocatalysis in non-aqueous environments. Future work should include multiple-site mutagenesis to explore combinatorial mutations based on flexible regions identified through MD that can further improve the thermal and solvent stability.

Acknowledgements
This research was supported by University Driven Research Program (Biotechnology and Biobased Industry).

Author contributions
U.U.M.J and S.N.H.I wrote the original draft, visualized, project administration, carried out the investigation, and formal analysis. W.L wrote, reviewed, and edited.R.N.Z.R.A.R, A.B.S and A.L.T.C validated, performed formal analysis, and data curation. M.S.M.A conceptualized, supervised, reviewed methodology, and data curation.

Data availability
All data supporting the findings of this study are available within the paper.

Declarations

Competing interests
The authors declare no competing interests.

Received: 17 July 2025 / Accepted: 27 September 2025
Published online: 27 October 2025

References

Abol-Fotouh D, AlHagar OE, Hassan MA (2021) Optimization, purification, and biochemical characterization of thermoalkaliphilic lipase from a novel *Geobacillus stearothermophilus* FMR12 for detergent formulations. Int J Biol Macromol 181. https://doi.org/10.1016/j.ijbiomac.2021.03.111

Al-Ghanayem AA (2021) Purification and characterization of thermo-alkaline stable lipase from *Bacillus coagulans* and its compatibility with commercially available detergents. Romania all Rights Reserved Rom Biotechnol Lett 26(5):2994–3001. https://doi.org/10.25083/rbl/26.5/2994.3001

Albayati SH, Masomian M, Ishak SNH, Ali MSBM, Thean AL, Shariff FBM, Noor NDBM, Rahman RNZRA (2020) Main structural targets for engineering lipase substrate specificity. Catalysts 10(7). https://doi.org/10.3390/catal10070747

Almeida FL, Travalia BM, Goncalves IS, Forte MBS (2021) Biodiesel production by lipase-catalyzed reactions: bibliometric analysis and study of trends. Biofuels Bioprod Biorefin 15(4):1141–1159. https://doi.org/10.1002/bbb.2183

Amalia MF, Hudiyono S, Setiasih S (2020) Inhibitor effect of PCMB and PMSF towards partially purified product from pineapple core (*Ananas comosus* [L.] Merr) using gel filtration column chromatography method. IOP Conf Ser Mater Sci Eng 902(1). https://doi.org/10.1088/1757-899X/902/1/012038

Basith S, Manavalan B, Shin TH, Lee G (2021) Mapping the intramolecular communications among different glutamate dehydrogenase States using molecular dynamics. Biomolecules 11(6). https://doi.org/10.3390/biom11060798

Bradford MM (1976) A rapid and sensitive method for the quantitation of microgram quantities of protein utilizing the principle of protein-dye binding. Anal Biochem 72(1–2). https://doi.org/10.1016/0003-2697(76)90527-3

Chemat F, Vian MA, Ravi HK, Khadhraoui B, Hilali S, Perino S, Tixier ASF (2019) Review of alternative solvents for green extraction of food and natural products: panorama, principles, applications and prospects. Molecules 24(16). https://doi.org/10.3390/molecules24163007

Drici N (2023) The influence of the hydrogen-bond network on the structure and dynamics of the RAPRKKG heptapeptide and its mutants. J Mol Graph Model 125. https://doi.org/10.1016/j.jmgm.2023.108598

Eltaweel MA, Rahman RNZRA, Salleh AB, Basri M (2005) An organic solvent-stable lipase from *Bacillus* sp. strain 42. Ann Microbiol 55(3)

García-Carreño FL (1992) Protease inhibition in theory and practice. Biotechnol Educ 3(4)

Guo X, Hu F, Zhao S, Yong Z, Zhang Z, Peng N (2022) Immunomagnetic separation method integrated with the Strep-tag II system for rapid enrichment and mild release of exosomes. Anal Chem. https://doi.org/10.1021/acs.analchem.2c03470

Hamid THA, Eltaweel MA, Rahman RNZRA, Basri M, Salleh AB (2009a) Characterization and solvent stable features of Strep-tagged purified recombinant lipase from thermostable and solvent tolerant *Bacillus* sp. strain 42. Ann Microbiol 59(1):111–118. https://doi.org/10.1007/BF03175607

Hamid THA, Rahman RNZRA, Salleh AB, Basri M (2009b) The role of lid in protein-solvent interaction of the simulated solvent stable thermostable lipase from *Bacillus* strain 42 in water-solvent mixtures. Biotechnol Biotechnol Equip 23(4). https://doi.org/10.2478/V10133-009-0015-5

Irianto VS, Demirkan E, Cetinkaya AA (2024) UV mutagenesis for lipase overproduction from *Bacillus cereus* ATA179, nutritional optimization, characterization and its usability in the detergent industry. Prep Biochem Biotechnol 54(7):918–931. https://doi.org/10.1080/10826068.2023.2299441

Ishak SNH, Masomian M, Kamarudin NHA, Ali MSM, Leow TC, Rahman RNZRA (2019) Changes of thermostability, organic solvent, and pH stability in *Geobacillus zalihae* HT1 and its mutant by calcium ion. Int J Mol Sci 20(10). https://doi.org/10.3390/ijms20102561

Jumper J, Evans R, Pritzel A, Green T, Figurnov M, Ronneberger O, Tunyasuvunakool K, Bates R, Žídek A, Potapenko A, Bridgland A, Meyer C, Kohl SAA, Ballard AJ, Cowie A, Romera-Paredes B, Nikolov S, Jain R, Adler J, Hassabis D (2021) Highly accurate protein structure prediction with alphafold. Nature 596(7873). https://doi.org/10.1038/s41586-021-03819-2

Khan MT, Ali S, Zeb MT, Kaushik AC, Malik SI, Wei DQ (2020) Gibbs free energy calculation of mutation in PncA and RpsA associated with pyrazinamide resistance. Front Mol Biosci 7. https://doi.org/10.3389/fmolb.2020.00052
Krieger E, Vriend G, Spronk C (2013) YASARA–yet another scientific artificial reality application. YASARA Org 993
Kwon DY, Rhee JS (1986) A simple and rapid colorimetric method for determination of free fatty acids for lipase assay. J Am Oil Chemists' Soc 63(1). https://doi.org/10.1007/BF02676129
Laemmli UK (1970) Cleavage of structural proteins during the assembly of the head of bacteriophage T4. Nature 227(5259):680–685. https://doi.org/10.1038/227680a0
Lindahl E, Hess B, van der Spoel D (2001) GROMACS 3.0: a package for molecular simulation and trajectory analysis. J Mol Model 7(8). https://doi.org/10.1007/S008940100045
Maiangwa J, Hamdan SH, Ali M, Salleh MS, Rahman ABZRA, Shariff RN, F. M., Leow TC (2021) Enhancing the stability of *Geobacillus zalihae* T1 lipase in organic solvents and insights into the structural stability of its variants. J Mol Graph Model 105. https://doi.org/10.1016/j.jmgm.2021.107897
Martínez L (2015) Automatic identification of mobile and rigid substructures in molecular dynamics simulations and fractional structural fluctuation analysis. PLoS One 10(3):e0119264. https://doi.org/10.1371/journal.pone.0119264
Min K, Kim HT, Park SJ, Lee S, Jung YJ, Lee JS, Yoo YJ, Joo JC (2021) Improving the organic solvent resistance of lipase a from *Bacillus subtilis* in water–ethanol solvent through rational surface engineering. Bioresour Technol 337. https://doi.org/10.1016/j.biortech.2021.125394
Noby N, Auhim HS, Winter S, Worthy HL, Embaby AM, Saeed H, Hussein A, Pudney CR, Rizkallah PJ, Wells SA, Jones DD (2021) Structure and in silico simulations of a cold-active esterase reveals its prime cold-adaptation mechanism. Open Biol 11(12). https://doi.org/10.1098/rsob.210182
Ong SN, Kamarudin NHA, Shariff FM, Noor NDM, Ali MSM, Rahman RN (2023) Effects of alcohol concentration and temperature on the dynamics and stability of mutant *Staphylococcal* lipase. J Biomol Struct Dyn. https://doi.org/10.1080/07391102.2023.2282177
Padhi AK, Janežič M, Zhang KYJ (2022) Molecular dynamics simulations: principles, methods, and applications in protein conformational dynamics. Adv Protein Mol Struct Biol Methods. https://doi.org/10.1016/B978-0-323-90264-9.00026-X
Paitaid P, Buatong J, Phongpaichit S, H-Kittikun A (2021) Purification and characterization of an extracellular lipase produced by *Aspergillus oryzae* ST11 as a potential catalyst for an organic synthesis. Trends Sci 18(21). https://doi.org/10.48048/tis.2021.45
Qin Z, Li Y, Feng N, Fei X, Tian J, Xu L, Wang Y (2023) Modulating the performance of lipase-hydrogel microspheres in a micro water environment. Colloids Surf B 223. https://doi.org/10.1016/j.colsurfb.2023.113171
Qu P, Lazim R, Li D, Xu R, Wang F, Li X, Zhang Y (2024) Enhancing methanoltolerance of Thermomyces lanuginosus lipase by rational design and biodiesel productionthrough one-step feeding of methanol. Journal of Cleaner Production, 450,141949. https://doi.org/10.1016/j.jclepro.2024.141949
Radkiewicz JL, Brooks CL (2000) Protein dynamics in enzymatic catalysis: exploration of dihydrofolate reductase. J Am Chem Soc 122(2). https://doi.org/10.1021/ja9913838
Salgado CA, dos Santos CIA, Vanetti MCD (2022) Microbial lipases: propitious biocatalysts for the food industry. Food Biosci 45. https://doi.org/10.1016/j.fbio.2021.101509
Shehata M, Timucin E, Venturini A, Sezerman OU (2020) Understanding thermal and organic solvent stability of thermoalkalophilic lipases: insights from computational predictions and experiments. J Mol Model 26(6). https://doi.org/10.1007/s00894-020-04396-3
Suhre K, Sanejouand YH (2004) ElNémo: A normal mode web server for protein movement analysis and the generation of templates for molecular replacement. Nucleic Acids Res 32. https://doi.org/10.1093/nar/gkh368
Veno J, Rahman RNZRA, Masomian M, Ali MSM, Kamarudin NHA (2019) Insight into improved thermostability of cold-adapted *Staphylococcal* lipase by glycine to cysteine mutation. Molecules 24(17). https://doi.org/10.3390/molecules24173169
Wand AJ, Sharp KA (2018) Measuring entropy in molecular recognition by proteins. Annual Rev Biophys 47. https://doi.org/10.1146/annurev-biophys-060414-034042
Xing S, Zhu R, Cheng K, Cai Y, Hu Y, Li C, Zeng X, Zhu Q, He L (2021) Gene expression, biochemical characterization of a sn-1, 3 extracellular lipase from *Aspergillus niger* GZUF36 and its model-structure analysis. Front Microbiol 12. https://doi.org/10.3389/fmicb.2021.633489
Zhang Y, Sun W, Elfeky NM, Wang Y, Zhao D, Zhou H, Wang J, Bao Y (2020) Self-assembly of lipase hybrid nanoflowers with bifunctional Ca^{2+} for improved activity and stability. Enzyme Microb Technol 132. https://doi.org/10.1016/j.enzmictec.2019.109408
Zhao J, Liu S, Gao Y, Ma M, Yan X, Cheng D, Wan D, Zeng Z, Yu P, Gong D (2021) Characterization of a novel lipase from *Bacillus licheniformis* NCU CS-5 for applications in detergent industry and biodegradation of 2,4-D Butyl ester. Int J Biol Macromol 176. https://doi.org/10.1016/j.ijbiomac.2021.01.214

Publisher's note